Bangladesh Pharmaceutical Journal ***26****(2): 167-184, 2023 (July)*

Bioactive Secondary Metabolites to Combat Diabetic Complications: Evidenced from *in Silico* Study

Hasin Hasnat[1], Suriya Akter Shompa[1], Fahmida Tasnim Richi[2], Md. Mirazul Islam[1], Mehedi Hasan Suman[1], Nazim Uddin Ahmed[3], Sania Ashrafi[2], Anika Zaman[1], Tanoy Saha[1], Md. Ashraful Islam[1] and Safaet Alam[3]

[1]Department of Pharmacy, State University of Bangladesh, Dhaka-1205, Bangladesh
[2]Department of Pharmaceutical Chemistry, Faculty of Pharmacy, University of Dhaka Dhaka-1000, Bangladesh
[3]Drugs and Toxins Research Division, BCSIR Laboratories Rajshahi, Bangladesh Council of Scientific and Industrial Research, Rajshahi-6206, Bangladesh

(Received: March 14, 2023; Accepted: June 22, 2023; Published (web): July 25, 2023)

Abstract

Diabetes mellitus (DM) is a condition characterized by excessive blood sugar levels, which have recently reached the level of a pandemic. There are various side effects of each drug to treat this condition. Molecular docking is a modern concept for computer-aided drug designing. Using this technique several potential antidiabetic phytocompounds are evaluated against three target receptors including GLUT-3, PPARγ and α-amylase related to DM. These compounds' ADMET and drug-likeliness characteristics have also been assessed to determine potential drug candidacy. Most of the compounds exhibited magnificent binding affinity against these targets, especially compounds 30 and 27 have shown great affinity against GLUT-3 with values of -11.2 and -10.2 Kcal/mol respectively. Where compound 37 has the highest binding affinity (-9.1 Kcal/mol) against PPARγ. Also, with values of -11.6 and -10.8 Kcal/mol respectively compounds 38 and 12 notably bind with α-amylase. Moreover, all of these compounds have magnificent results on ADMET and drug-likeliness studies, in particular, compound 29 has shown high affinity against all of these receptors, explored 0.55% bioavailability score, no toxicity and high absorptivity. Although these compounds have undergone a preliminary drug discovery study, more research must be done to determine their precise mechanism of action against DM.

Key words: Antidiabetic, phytochemical, *in silico*, molecular docking, ADMET, GLUT-3, PPARγ, α-amylase.

Introduction

A well-known chronic metabolic condition is diabetes mellitus, which is characterized by insufficient insulin secretion and/or activity. A lack of insulin, an anabolic hormone, can cause abnormalities in the metabolism of proteins, carbs and lipids (HM *et al.*, 2015). Metabolic diseases can be greatly impacted by low insulin levels, insulin resistance in target tissues, insulin-receptor expression, particularly in adipose tissue and skeletal muscles, and to a lesser extent in the liver, effector enzymes, and/or signal transduction system (Amraee and Bahramikia, 2019). One of the most prevalent metabolic disorders in the world, diabetes affects roughly 2.8% of people worldwide and is expected to reach 4.4% by 2030, reaching an epidemic level that has never been seen before (Becheva and Kirkova-Bogdanova, 2022). Bangladesh is seeing an increase in the prevalence of diabetes. According to the International Centre for Diarrhoeal Disease Research in Bangladesh, 7.1 million persons had diabetes in 2015, while an additional 3.7 million cases went undetected and around 129,000 deaths were associated with the diabetic condition. The incidence of diabetes has increased 2.5 times in the last 20 years, from 4.0% in 1995-2000 to 10.4% in 2010-2019 (Alam *et al.*,

Corresponding author: Safaet Alam; E-mail: safaet.du@gmail.com
DOI: https://doi.org/10.3329/bpj.v26i2.67807

2022b). Various classes of oral hypoglycemic drugs are currently available for therapeutic usage, each with a unique profile of side effects. For the medical system, managing diabetes without any side effects remains a problem. The demand for natural products with antidiabetic action and minimal side effects rises as a result (Balamurugan *et al.,* 2012).

Plants are a reliable source of necessary medical substances (Emon *et al.,* 2021a, Kabir *et al.,* 2021; Asad *et al.,* 2022). Before the development of modern medicines, people made predictions about the therapeutic potential of medicinal plants (Alam *et al.,* 2020). To cure different medical diseases, both conventional and unconventional approaches are frequently used worldwide (Alam *et al.,* 2021a; Chowdhury *et al.,* 2022). Natural plant-based products have recently drawn attention as a substantial source of cutting-edge, safe and potent secondary bioactive metabolites with therapeutic promise (Obonti *et al.,* 2021). Plant-based medicines are expected to account for up to 25% of all medications in established countries like the United States, while they will account for over 80% of all medications in quickly developing countries like India and China (Islam *et al.,* 2022a). On the planet, there are 400,000 secondary plant metabolites, yet only 10,000 of them have been chemically isolated, according to conservative estimates (Islam *et al.,* 2022b). Phytochemicals, which are also the main pharmacological substances found in plants, are the main sources of novel medications (Alam *et al.,* 2020; Emon *et al.,* 2021b). The pharmacological activity and associated mechanisms of action of these phytochemicals are established by a number of experimental methodologies, including *in vitro, in vivo* and *in silico* research, etc. (Emon *et al.,* 2020a; Islam *et al.,* 2022b; Chakrabarti *et al.,* 2022; Ashrafi *et al.,* 2022).

One such structure-driven drug development technique is molecular docking, which predicts molecular interactions and forecasts the binding mechanism and affinity between receptors and ligands. This technology has been heavily utilized recently in the realm of drug design research. Researchers can easily acquire, manufacture and execute follow-up pharmacological tests by using the chemicals database to screen possible pharmacophores, which also considerably increases efficiency and lowers research costs (Fan *et al.,* 2019). Molecular docking has a wide range of uses and applications in drug discovery, including structure-activity investigations, lead optimization, discovering potential leads through virtual screening, delivering binding hypotheses to facilitate predictions for mutagenesis studies, supporting x-ray crystallography in the integrating of substrates as well as inhibitors to electron density, chemically based mechanism experiments and combinatorial library design (Morris and Lim-Wilby, 2008).

In this article, the antidiabetic potential of several known antidiabetic phytochemicals has been investigated against some receptors through molecular docking to evaluate the binding ability and probable mechanism pathways of these compounds. Also, the ADMET and drug-likeliness have been investigated to identify the bioavailability and the drug-like candidacy of these phytocompounds.

Materials and Methods

Docking software: Some antidiabetic phytocompounds isolated from important medicinal plants mentioned in table 1 (Alam *et al.,* 2022a) were computationally docked using the well-known software programs PyRx, PyMoL 2.3, Discovery Studio 4.5, and Swiss PDB viewer.

Ligand preparation: All the compounds shown in table 1 were searched in the PubChem database (https://pubchem.ncbi.nlm.nih.gov/) and downloaded their 3D structure in SDF format. The structures of these compounds are shown in figure 1. Also, the 3D SDF structure of glibenclamide (PubChem CID-3488) and pioglitazone (PubChem CID- 4829) were downloaded as standard. These ligands and their PubChem CIDs were serially loaded in the discovery studio 4.5. It should be mentioned that the Pm6 semiempirical technique was used to optimize all phytochemicals in order to improve docking accuracy (Mahmud *et al.,* 2021).

Table 1. Commonly isolated phytocompounds reported to have antidiabetic activities and their PubChem CID.

SL	Compounds	Plant source	Family	Pub Chem CID	Formula
1	Ajoene	*Allium sativum*L	Amaryllidaceae	5386591	C9H14OS3
2	Isoorientin	*Cecropia obtusifolia* Bertol.	Urticaceae	114776	C21H20O11
3	Scutellarein	*Scoparia dulcis* L.	Scrophulariaceae	5281697	C15H10O6
4	22-dihydroxyolean-12-en-29-oic acid	*Salacia chinensis* L.	Celastraceae	127707	C30H48O4
5	Aegeline	*Aegle marmelos* Correa	Rutacea	15558419	C18H19NO3
6	Allicin	*Allium sativum*L	Amaryllidaceae	65036	C6H10OS2
7	Alliin	*Allium sativum*L	Amaryllidaceae	87310	C6H11NO3S
8	Allyl mercaptan	*Allium sativum*L	Amaryllidaceae	13367	C3H6S
9	Apigenin	*Scoparia dulcis* L.	Scrophulariaceae	5280443	C15H10O5
10	Apigenin 8-C-β-D glucopyranoside (vitexin)	*Beta vulgaris* L.	Chenopodiaceae	5280441	C21H20O10
11	Asiatic acid	*Centella asiatica* (L.) Urb.	Apiaceae	119034	C30H48O5
12	Asiaticoside (triterpene saponin compound)	*Centella asiatica* (L.) Urb.	Apiaceae	11954171	C48H78O19
13	Betulinic acid	*Scoparia dulcis* L.	Scrophulariaceae	64971	C30H48O3
14	Butyl-isobutyl-phthalate	*Laminaria japonica* Aresch.	Laminariaceae	28813	C16H22O4
15	Caffeic acid	*Artocarpus heterophyllus* Lam	Moraceae	689043	C9H8O4
16	Catechin	*Artocarpus heterophyllus* Lam	Moraceae	9064	C15H14O6
17	Chlorogenic acid	*Cecropia obtusifolia* Bertol.	Urticaceae	1794427	C16H18O9
18	Corosolic acid	*Lagerstroemia speciosa* (L.) Pers.	Lythraceae	6918774	C30H48O4
19	Diallyl trisulfide	*Allium sativum*L	Amaryllidaceae	16315	C6H10S3
20	D-pinito	*Bougainvillea spectabilis* Willd.	Nyctaginaceae	164619	C7H14O6
21	Gallic acid	*Artocarpus heterophyllus* Lam	Moraceae	370	C7H6O5
22	Kaempferitrin	*Bauhinia forficate* Link	Fabaceae	5486199	C27H30O14
23	Kaempferol	*Mangifera indica* L	Anacardiaceae	5280863	C15H10O6
24	Kotalanol	*Salacia reticulata* Wight	Celastraceae	42632210	C12H24O12S2
25	Luteolin	*Scoparia dulcis* L.	Scrophulariaceae	5280445	C15H10O6
26	Madecassic acid	*Centella asiatica* (L.) Urb.	Apiaceae	73412	C30H48O6
27	Mangiferin	*Mangifera indica* L	Anacardiaceae	5281647	C19H18O11
28	Quercetin	*Artocarpus heterophyllus* Lam	Moraceae	5280343	C15H10O7
29	Regeol A	*Salacia chinensis* L.	Celastraceae	10694409	C28H40O4
30	Rutin	*Artocarpus heterophyllus* Lam	Moraceae	5280805	C27H30O16
31	Salacinol	*Salacia reticulata* Wight	Celastraceae	6451151	C9H18O9S2
32	Salasol A	*Salacia chinensis* L.	Celastraceae	11092680	C28H36O10
33	S-allyl cysteine	*Allium sativum*L	Amaryllidaceae	9793905	C6H11NO2S
34	Scopadulcic acid B	*Scoparia dulcis* L.	Scrophulariaceae	11729855	C27H34O5
35	Scoparic acid A	*Scoparia dulcis* L.	Scrophulariaceae	44584621	C27H36O5
36	Stevioside	*Stevia rebaudiana* Bertoni	Asteraceae	442089	C38H60O18
37	Tingenone	*Salacia chinensis* L.	Celastraceae	101520	C28H36O3
38	Triptocalline A	*Salacia chinensis* L.	Celastraceae	44559634	C28H42O4

Receptor preparation: The 3D structure of glucose transporter 2 or GLUT2 [PDB ID: 4ZWB] (Mojica *et al.,* 2017), peroxisome proliferator-activated receptor gamma or PPARγ [PDB ID: 4EMA] (Selvaraj *et al.,* 2014), and alpha-amylase [PDB ID 1HNY] (Jhong *et al.,* 2015) were downloaded from the protein data bank (https://www.rcsb.org). The PDB format was used to store all the proteins and receptors. Running the obtained proteins via PyMoL 2.3 rendered them water

and ligand/residue free. After that, all of the biomolecules were ordered by adding non-polar hydrogen atoms and retained in their lowest energy state by using a Swiss PDB viewer energy minimization tool.

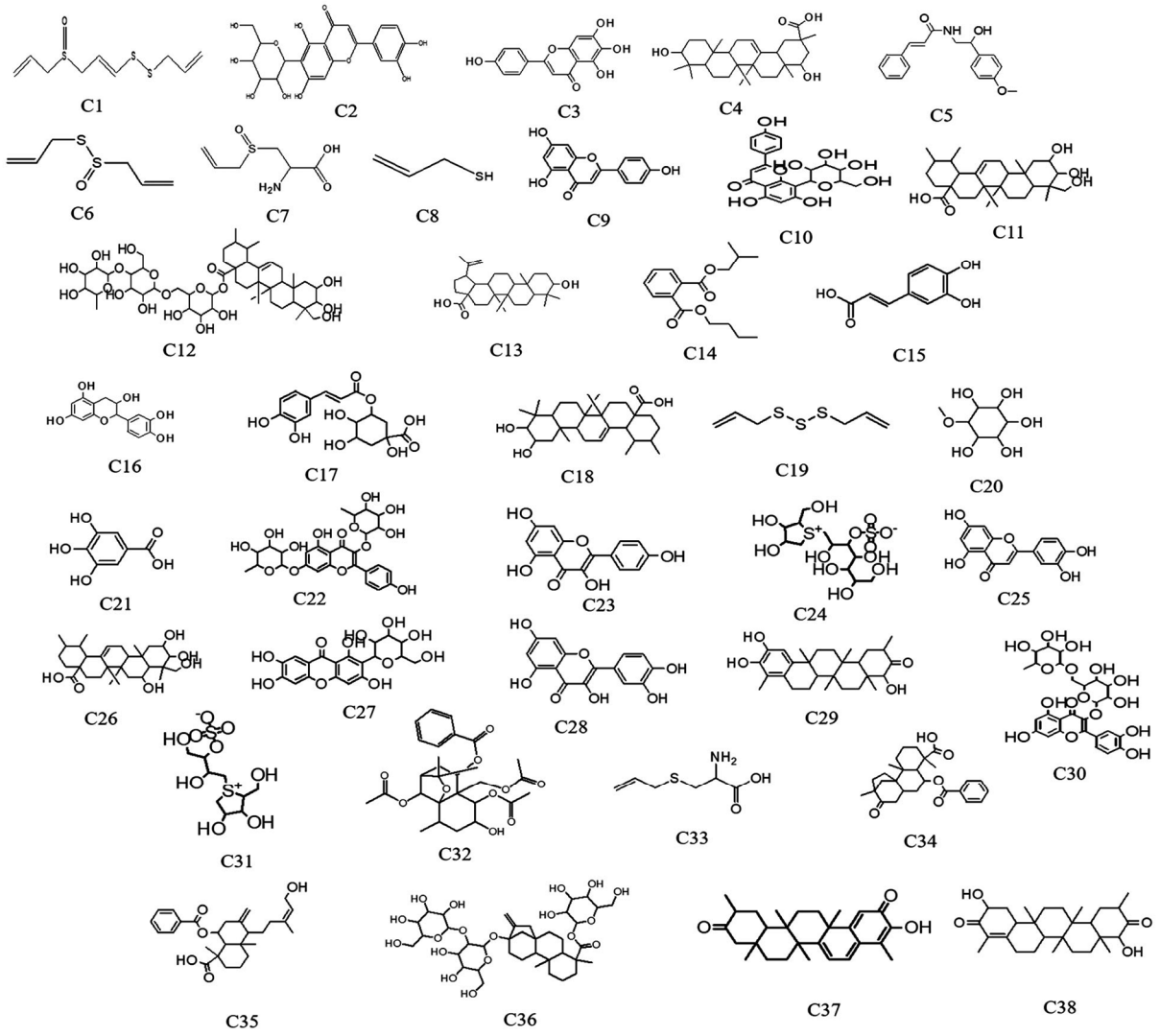

Figure 1. Structures of the isolated phytocompounds used for molecular docking.

Results and Discussion

Ligand-receptor binding: To forecast potential binding profiles of phytocompounds with their affinities to the target molecules, the current computer-aided ligand-protein interaction has been drawn. A highly sophisticated PyRxAutodock Vina was used for this molecular drug-protein linking procedure, and semiflexible modelling was used for the molecular docking. First, the protein has been loaded and formatted to the desired macromolecule, and the literature-based amino acids with their ID have been chosen to ensure that the ligands bind to the desired macromolecule only. For 4ZWB targets TYR26, THR28, GLY29, VAL30, LEU167, THR191, PRO194, GLN198, ILE309, GLY312, VAL313, THR347, TRP410, LEU418 and PHE442 were selected for site targeting docking (Mojica *et al.*, 2017). However ILE-281, GLY-284, CYS-285, SER-

289, HIS-323, TYR-327, MET-364, HIS-449 and TYR-473 were picked for the B chain of 4EMA target (Selvaraj *et al.*, 2014), as well as, TRP-59, TRY-151, LEU-162, THR-163, ALA-198, LYS-200, GLU-233, ASP-300, HIS-305 was chosen for target site of 1HNY (Jhong *et al.*, 2015). Glibenclamide (PubChem CID- 3488) was used as the standard against GLUT-3 and α-amylase while pioglitazone (PubChem CID-4829) was used against PPARγ. Additionally, to match the best optimal hit during the docking against these selected macromolecules, all the PDB files of the ligands were imported and afterwards minimized into pdbqt format with the Open Bable tool in the PyRxAutoDock Vina software. Moreover, the grid box was created by maintaining the protein's active binding sites inside of the box, which was designated by the grid mapping. The Center X = 106.702644121, Y = 10.6511712781 and Z = 60.5557720536, and Dimension X = 45.6772718548, Y = 24.508706425, and Z = 33.274481395 were kept during GLUT2 docking. For PPARγ the grid box was maintained Center X = -4.09130393668, T = -15.5556423812, Z = 21.357516045, and Dimension X = 23.9896362426, Y = 18.7244959435, and Z = 23.3355168288 Beside Center X = 9.37765799237, Y = 43.6599343537, Z = 21.1019192615, and Dimesnion X = 24.0100362347, Y = 19.1934569044 and Z = 20.5856600056 were fixed as grid box for α-amylase docking. During docking, the remaining parameters were set to their default values. Then, using AutoDock Vina (version 1.1.2), computer-aided molecular docking of the ligands was carried out while maintaining all relevant conditions. Finally, BIOVIA Discovery Studio version 4.5 was used to conceptualize all docking investigations for predicting the best-fitted models using 2D and 3D arrangements.

Pharmacokinetic (ADMET) and drug-likeliness analysis: Nowadays, pharmacokinetic (absorption, distribution, metabolism, excretion and toxicology) and bioavailability study through drug-likeliness determination are becoming popular in computer-based drug design. From the standpoint of drug discovery, ADMET analyses are utilized to figure out the pharmacological structure (http://biosig.unimelb.edu.au/pkcsm/prediction). SwissADME (http://www.sib.swiss), an online program, was also used to predict drug likeliness (Lipinski rules) and pharmacokinetics for substances. According to Lipinski, an ingredient would be orally accessible if it met the following criteria: molecular weight < 500 amu, hydrogen bond donor sites < 5, hydrogen bond acceptor sites < 10, and lipophilicity value LogP ≤5 (Alam 2021b). Table manifested ADMET and drug likeliness results of these compounds.

Results and Discussion

In the past, there have been a number of mechanisms of action associated with the antidiabetic effects including inhibition of α-glucosidase, an enzyme secreted from the brush border of the small intestine that aids in carbohydrate digestion; inhibition of the dipeptidyl peptidase-4 (DPP-4) enzyme, which stimulates insulin secretion and inhibits glucagon secretion; inhibition of α-amylase, an enzyme secreted from salivary glands that reduced breakdown of glycogen and starch; increased secretion of insulin through increasing intracellular calcium ion [Ca2+]i and stimulating pancreatic β cells; improvement of the hormone glucagon-like peptide-1 (GLP-1), which increases insulin secretion, and last but not least, regulation of the glucose transporter type 4 (GLUT-4) have been mentioned as ways to increase insulin secretion are described (Alam *et al.*, 2022b).

Three common receptors namely GLUT-3, PPARγ, and α-amylase were selected and the computer-aided molecular modelling analysis was carried out using the appropriate tools in order to clearly and better comprehend the molecular impacts of these isolated natural compounds (Table 1) on the aforementioned biological target.

For GLUT-3 most of the compounds exhibited notable binding affinity, however, compounds 30 and 27 manifested magnificent binding affinity of -11.2 Kcal/mol and -10.2 Kcal/mol respectively which exceeded standard glibenclamide (-10.1 Kcal/mol). Compound 22 showed affinity against GLUT-3 with a value of -9.8 Kcal/mol, and compound 25 showed -9.6 Kcal/mol. Additionally, satisfactory -9.4 Kcal/mol

Table 2. Molecular docking results of 38 compounds and two standards against three targets.

Compounds	Binding affinity (Kcal/mol)		
	GLUT-3	PARP-γ	α-Amylase
C1	-5	-4.6	-4.3
C2	-8.9	-7.5	-8.3
C3	-9.4	-7.6	-8.4
C4	-8.2	-8.2	-9.3
C5	-8.6	-7.6	-7.7
C6	-4.5	-4.2	-3.6
C7	-5.5	-4.3	-4.7
C8	-2.7	-2.6	-2.4
C9	-9.3	-7.6	-8.6
C10	-9.3	-7.7	-8.4
C11	-7.7	-7.2	-9
C12	-7.5	-3.8	-10.8
C13	-8.1	-7.4	-9.7
C14	-7.3	-6.7	-6.1
C15	-6.8	-6.1	-6.4
C16	-9.4	-7.3	-8.6
C17	-9.4	-8	-7.4
C18	-8.6	-7.4	-10
C19	-4.1	-3.5	-3.4
C20	-6	-4.6	-5.5
C21	-6.9	-5.6	-5.9
C22	-9.8	-8.7	-8.4
C23	-9.2	-7.1	-8.4
C24	-7.2	-5.6	-6
C25	-9.6	-8	-8.6
C26	-7.9	-7	-9.1
C27	-10.2	-7.3	-8.3
C28	-9.4	-7.2	-8.7
C29	-9.3	-8.3	-9.9
C30	-11.2	-8.2	-8.9
C31	-7.3	-5.6	-6.2
C32	-6.5	-7.1	-7.8
C33	-4.9	-4.3	-4.6
C34	-8.9	-8.5	-10.5
C35	-7.4	-7.2	-8.7
C36	-8.8	-8.3	-8.8
C37	-8.7	-9.1	-10.5
C38	-8.8	-7.5	-11.6
Glibenclamide	-10.1	-	-8.9
Pioglitazone	-	-7.3	-

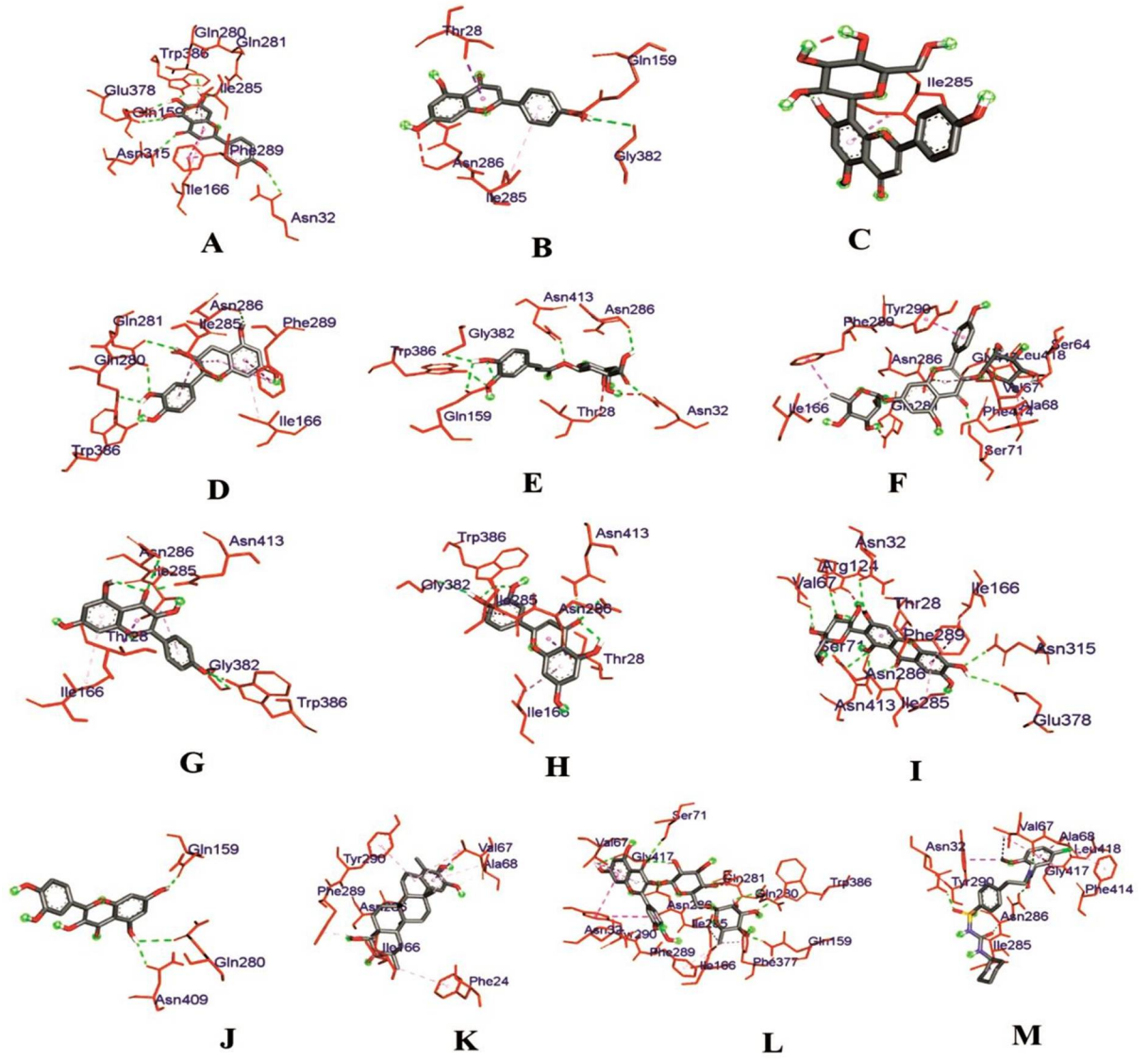

Figure 2. Graphical representation of the molecular interactions of the most prominent phytocompounds with the GLUT-3 (PDB ID: 4ZWB) enzyme with 3D visualization (Compound 3 = A, Compound 9 = B, Compound 10 = C, Compound 16 = D, Compound 17 = E, Compound 22 = F, Compound 23 = G, Compound 25 = H, Compound 27 = I, Compound 28 = J, Compound 29 = K, Compound 30 = L, and Standard Glibenclamide = M).

affinity was observed for compounds 3, 16, 17 and 28, as well as -9.3 Kcal/mol was observed for compounds 9, 10, and 29 (Table-2). Compound 27 attached to 12 amino acids of GLUT-3 including THR-28, ASN-32, VAL-67, SIR-71, ARG-124, ILE-168, ILE-285, ASN-286, PHE-289, ASN-315, GLU-318, and ASN-413; where the compound 30 bonded to 14 amino acids namely ASN-32, VAL-67, SER-71, GLN-159, ILE-166, GLN-280, GLN-281, ILE-285, ASN-286, PHR-289, TYR-289, TYR-290, PHE-377, TRP-386, AND GLY-417; compared to standard glibenclamide which bound with only 9 amino acids namely ASN-32, VAL-67, ALA-68, ILE-285, ASN-286, TYR-290, PHE-414, GLY-417 and LEU-418 (Figures 2 and 3).

For the target PPARγ, compounds 3, 9, 10, 17, 22, 25, 29 and 30 also exhibited prominent results with binding affinities of -7.6, -7.6, -7.7, -8, -8.7, -8,

Table 3. Absorption and distribution profile of the compounds.

Compounds	Absorption							Distribution			
	Water solubility (log mol/L)	Caco2 permeability (log Papp in 10-6 cm/s)	Intestinal absorption (human) (% Absorbed)	Skin permeability (log Kp)	P-glycoprotein substrate	P-glycoprotein I inhibitor	P-glycoprotein II inhibitor	VDss (human) (log L/kg)	Fraction unbound (human) (Fu)	BBB permeability	CNS permeability
C1	-3.54	1.329	95.186	-1.745	No	No	No	0.083	0.395	0.703	-2.178
C2	-2.9	-0.912	61.768	-2.735	Yes	No	No	1.603	0.219	-1.564	-3.939
C3	-3.156	-0.357	66.687	-2.735	Yes	No	No	0.587	0.192	-1.398	-2.363
C4	-4.017	0.695	92.398	-2.735	No	No	Yes	-0.981	0.034	-0.449	-1.408
C5	-3.311	1.245	93.228	-2.975	Yes	No	No	0.205	0.043	-0.098	-2.404
C6	-1.72	1.316	96.229	-1.877	No	No	No	-0.045	0.577	0.506	-2.312
C7	-2.888	0.619	76.495	-2.735	No	No	No	-0.553	0.462	-0.271	-3.472
C8	-0.887	1.385	100	-2.202	Yes	No	No	0.055	0.691	0.113	-2.307
C9	-3.329	1.007	93.25	-2.735	Yes	No	No	0.822	0.147	-0.734	-2.061
C10	-2.845	-0.956	46.695	-2.735	Yes	No	No	1.071	0.242	-1.449	-3.834
C11	-3.008	0.479	62.855	-2.735	No	No	No	-1.6	0.119	-0.646	-1.984
C12	-2.874	-1.104	29.201	-2.735	Yes	Yes	No	-0.578	0.402	-1.884	-5.247
C13	-3.122	1.175	99.763	-2.735	No	No	No	-1.18	0.018	-0.322	-1.343
C14	-4.277	1.667	95.035	-2.65	No	No	No	-0.071	0.124	-0.025	-2.303
C15	-2.33	0.634	69.407	-2.722	No	No	No	-1.098	0.529	-0.647	-2.608
C16	-3.117	-0.283	68.829	-2.735	Yes	No	No	1.027	0.235	-1.054	-3.298
C17	-2.449	-0.84	36.377	-2.735	Yes	No	No	0.581	0.658	-1.407	-3.856
C18	-3.04	0.641	100	-2.735	No	No	No	-1.282	0.037	-0.473	-1.507
C19	-3.781	1.403	92.573	-1.449	No	No	No	0.216	0.483	0.767	-2.309
C20	-1.401	-0.14	36.202	-2.997	No	No	No	-0.213	0.873	-1.053	-4.019
C21	-2.56	-0.081	43.374	-2.735	No	No	No	-1.855	0.617	-1.102	-3.74
C22	-2.964	0.225	35.385	-2.735	Yes	No	No	1.487	0.129	-1.823	-4.673
C23	-3.04	0.032	74.29	-2.735	Yes	No	No	1.274	0.178	-0.939	-2.228
C24	-2.745	-0.788	0	-2.735	Yes	No	No	-1.267	0.782	-2.077	-4.982
C25	-3.094	0.096	81.13	-2.735	Yes	No	No	1.153	0.168	-0.907	-2.251
C26	-3.037	0.455	57.113	-2.735	Yes	No	No	-1.555	0.181	-0.737	-2.944
C27	-2.918	-0.926	46.135	-2.735	Yes	No	No	1.364	0.289	-1.573	-4.211
C28	-2.925	-0.229	77.207	-2.735	Yes	No	No	1.559	0.206	-1.098	-3.065
C29	-3.858	0.671	94.799	-2.763	Yes	Yes	Yes	-0.034	0.052	-0.451	-1.557
C30	-2.892	-0.949	23.446	-2.735	Yes	No	No	1.663	0.187	-1.899	-5.178
C31	-1.98	-0.52	0	-2.735	Yes	No	No	-1.337	0.756	-1.266	-3.944
C32	-5.158	1.029	95.352	-2.754	No	Yes	No	-0.063	0.065	-1.314	-3.026
C33	-2.888	0.704	79.971	-2.736	No	No	No	-0.561	0.444	-0.277	-3.417
C34	-3.882	0.579	99.15	-2.735	No	No	Yes	-0.964	0	-0.186	-1.87
C35	-4.27	0.629	96.454	-2.734	Yes	No	Yes	-1.074	0	0	-2.093
C36	-2.468	-1.087	0	-2.735	Yes	No	No	-0.62	0.477	-2.029	-5.56
C37	-6.06	1.281	94.801	-3.302	No	Yes	Yes	0.127	0	0.041	-1.184
C38	-4.994	0.606	96.235	-3.115	No	Yes	Yes	-0.417	0	0.182	-1.665

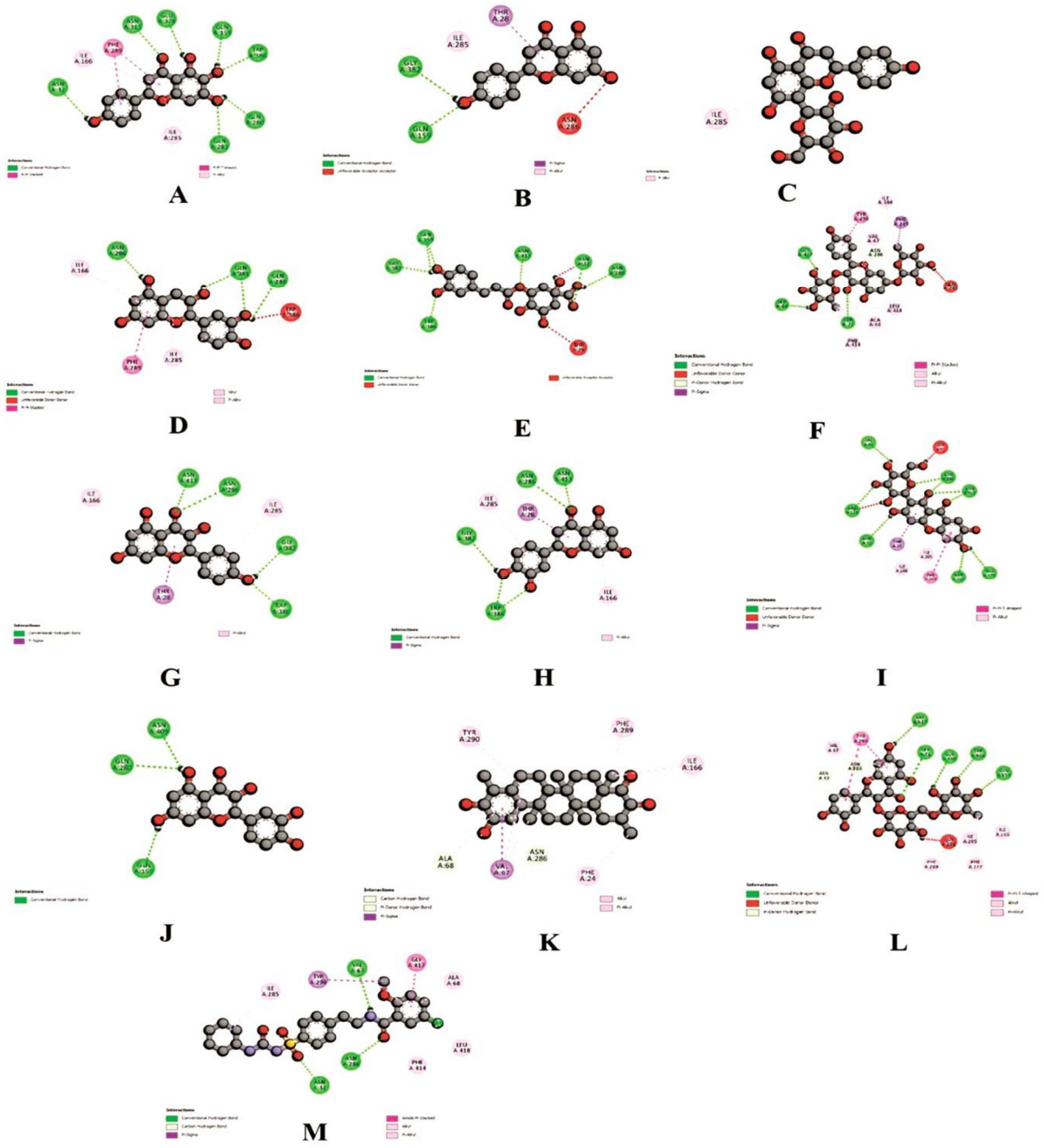

Figure 3. Graphical representation of the molecular interactions of the most prominent phytocompounds with the GLUT-3 (PDB ID: 4ZWB) enzyme with 2D visualization (Compound 3 = A, Compound 9 = B, Compound 10 = C, Compound 16 = D, Compound 17 = E, Compound 22 = F, Compound 23 = G, Compound 25 = H, Compound 27 = I, Compound 28 = J, Compound 29 = K, Compound 30 = L, and standard glibenclamide = M).

Table 4. Metabolism and excretion profile of the compounds.

Compounds	Metabolism							Excretion	
	CYP2D6 substrate	CYP3A4 substrate	CYP1A2 inhibitor	CYP2C19 inhibitor	CYP2C9 inhibitor	CYP2D6 inhibitor	CYP3A4 inhibitor	Total clearance (log ml/min/kg)	Renal OCT2 substrate
C1	No	No	No	No	No	No	No	0.538	No
C2	No	No	No	No	No	No	No	0.372	No
C3	No	No	Yes	No	No	No	No	0.47	No
C4	No	Yes	No	No	No	No	No	0.006	No
C5	No	Yes	Yes	Yes	No	No	No	0.353	No
C6	No	No	No	No	No	No	No	0.714	No
C7	No	No	No	No	No	No	No	0.365	No
C8	No	No	No	No	No	No	No	0.359	No
C9	No	No	Yes	Yes	No	No	No	0.566	No
C10	No	No	No	No	No	No	No	0.444	No
C11	No	Yes	No	No	No	No	No	0.202	No
C12	No	No	No	No	No	No	No	0.227	No
C13	No	Yes	No	No	No	No	No	0.116	No
C14	No	Yes	Yes	Yes	No	No	No	0.877	No
C15	No	No	No	No	No	No	No	0.508	No
C16	No	No	No	No	No	No	No	0.183	No
C17	No	No	No	No	No	No	No	0.307	No
C18	No	Yes	No	No	No	No	No	0.093	No
C19	No	No	No	No	No	No	No	0.446	No
C20	No	No	No	No	No	No	No	0.659	No
C21	No	No	No	No	No	No	No	0.518	No
C22	No	No	No	No	No	No	No	-0.102	No
C23	No	No	Yes	No	No	No	No	0.477	No
C24	No	No	No	No	No	No	No	2.006	No
C25	No	No	Yes	No	Yes	No	No	0.495	No
C26	No	Yes	No	No	No	No	No	0.212	No
C27	No	No	No	No	No	No	No	0.347	No
C28	No	No	Yes	No	No	No	No	0.407	No
C29	No	Yes	No	Yes	No	No	No	-0.005	No
C30	No	No	No	No	No	No	No	-0.369	No
C31	No	No	No	No	No	No	No	0.959	No
C32	No	Yes	No	No	No	No	No	0.67	No
C33	No	No	No	No	No	No	No	0.591	No
C34	No	Yes	No	No	No	No	No	0.252	No
C35	No	Yes	No	No	No	No	No	0.901	No
C36	No	No	No	No	No	No	No	0.691	No
C37	No	Yes	No	No	No	No	No	0.064	No
C38	No	Yes	No	No	No	No	No	0.238	No

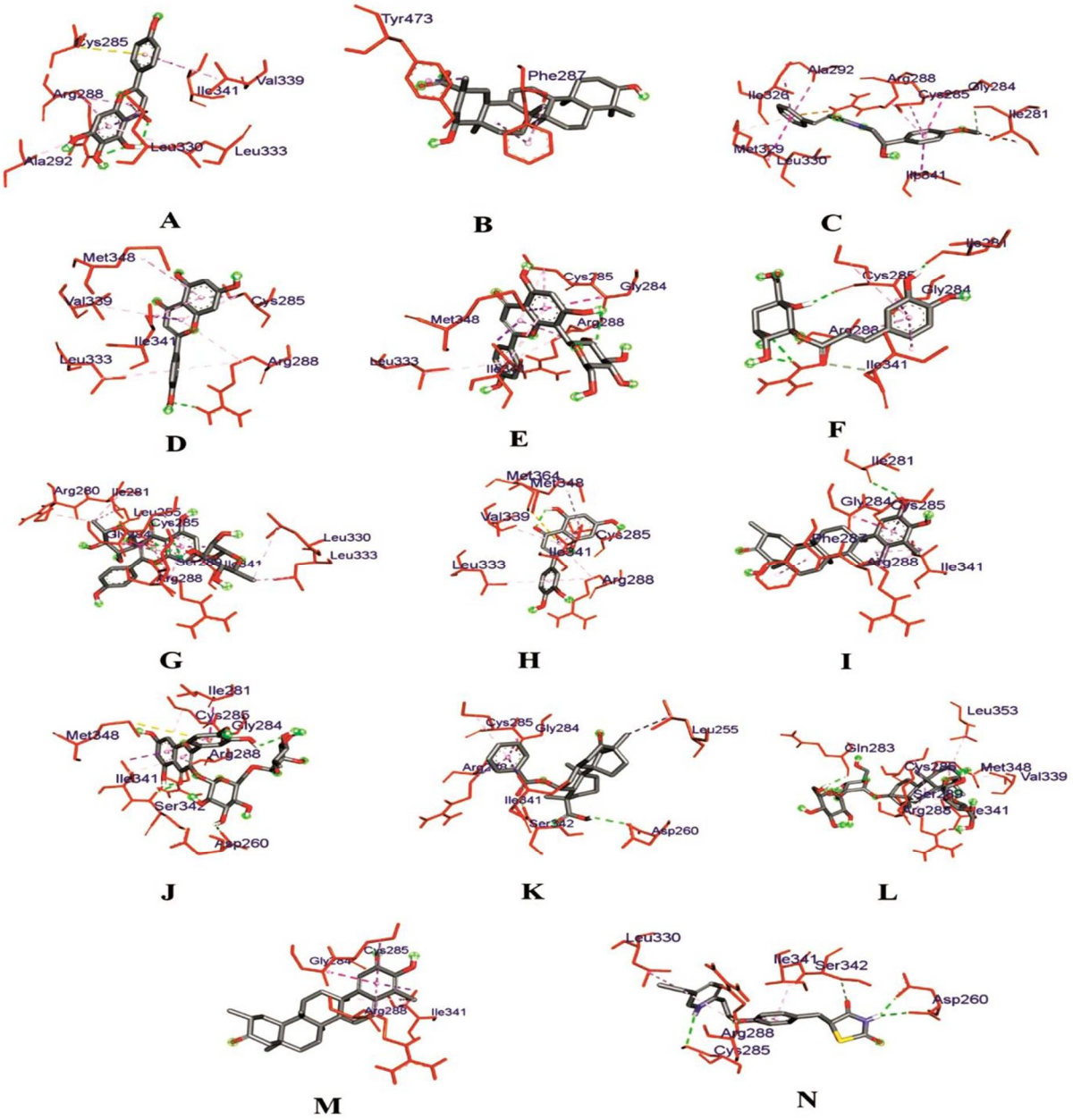

Figure 4. Graphical representation of the molecular interactions of the most promising phytocompounds with the PPARγ (PDB ID: 4EMA) enzyme with 3D visualization (Compound 3 = A, Compound 4 = B, Compound 5 = C, Compound 9 = D, Compound 10 = E, Compound 17 = F, Compound 22 = G, Compound 25 = H, Compound 29 = I, Compound 30 = J, Compound 34 = K, Compound 36 = L, Compound 37 = M and standard pioglitazone = N).

-8.3, and -8.2 Kcal/mol respectively compared to standard pioglitazone -7.3 Kcal/mol. Moreover, the highest binding affinity was manifested by compound 37 with a value of -9.1 Kcal/mol (Table 2). The standard was bound the active sites including ASP-260, CYS-285, ARL-288, LEU-330, ILE-341, and SER-342; while the compound 37 was attached with GLY-284, CYS-285, ARG-288, and ILE-341. Also, compound 22 (second highest affinity) conjugated to 10 amino acids of PPARγ, which includes LEU-255, ARG-280, ILE-281, GLY-284, CYS-285, ARG-288,

SER-289, LEU-330, LEU-333 and ILE-341 (Figures 4 and 5).

By binding with 9 amino acids of α-amylase namely, TRP-58, TRP-59, TYR-62M GLN-63, LEU-162, ALA-198, LYS-200, HIS-201 and ILE-235 the compound 38 exhibited the highest binding affections of -11.6 Kcal/mol, where the second highest affinity (-10.8 Kcal/mol) against the receptor was observed for compound 12 which bonded with 11 amino acids, that is ILE-51, TRP-59, VAL-107, TYR-151, ARG-195, ASP-197, GLU-233, ILE 235, ASP-300, HIS-305 and ALA-307 in comparison the standard

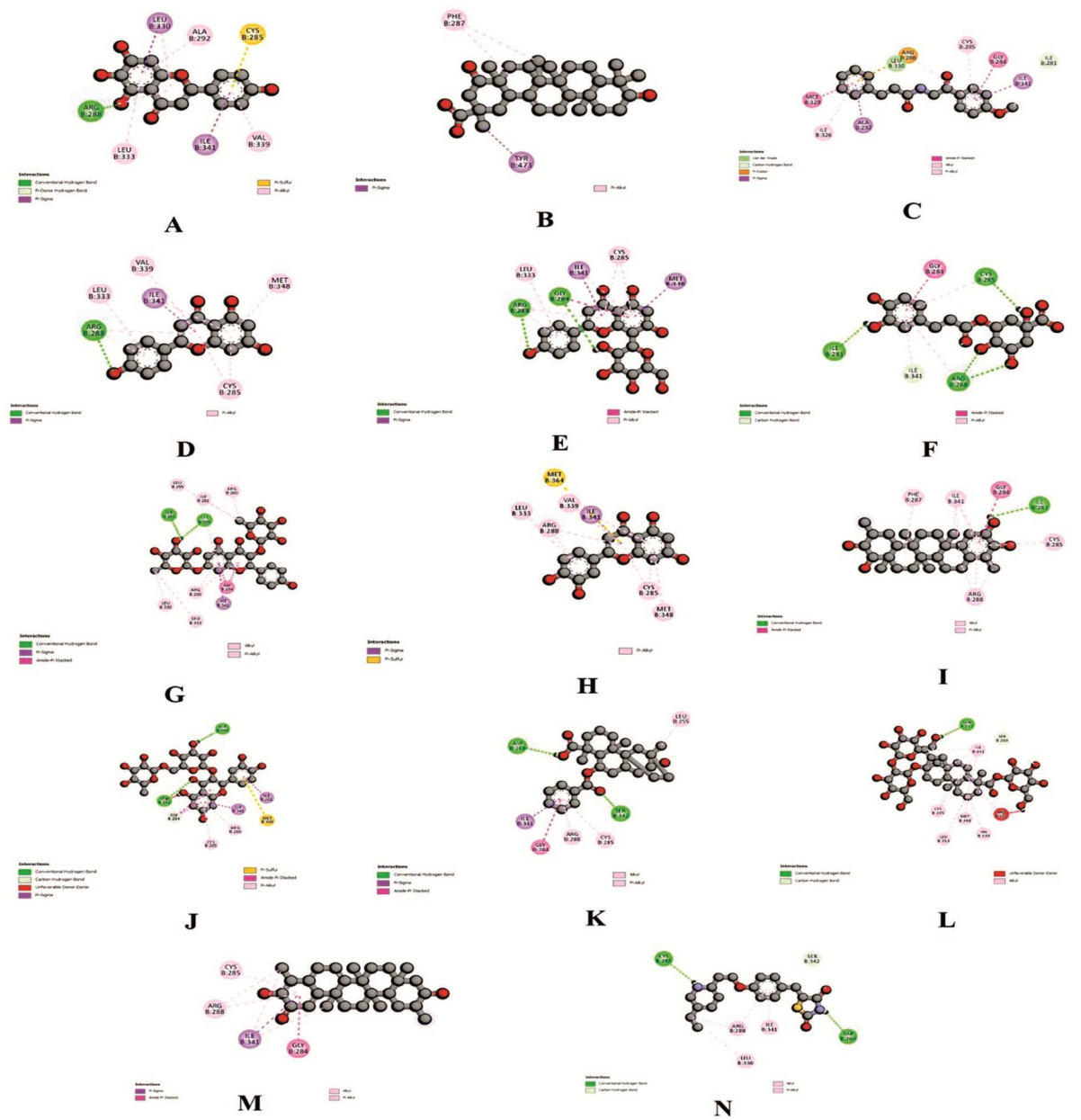

Figure 5. Graphical representation of the molecular interactions of the most promising phytocompounds with the PPARγ (PDB ID: 4EMA) enzyme with 2D visualization (Compound 3 = A, Compound 4 = B, Compound 5 = C, Compound 9 = D, Compound 10 = E, Compound 17 = F, Compound 22 = G, Compound 25 = H, Compound 29 = I, Compound 30 = J, Compound 34 = K, Compound 36 = L, Compound 37 = M and standard pioglitazone = N).

Table 5. Toxicological profile and drug-likeliness study through Lipinski's rule of five (MW ≤ 500, MLOGP ≤ 4.15, N or O ≤ 10, NH or OH ≤ 5 and Log Po/w ≤ 5) of the compounds.

	Toxicity											Drug-likeness
Compounds	AMES toxicity	Max. tolerated dose (human) (log mg/kg/day)	h ERG I inhibitor	hERG II inhibitor	Oral rat acute toxicity (LD50) (mol/kg)	Oral rat chronic toxicity (LOAEL) (log mg/kg_bw/day)	Hepatotoxicity	Skin sensitisation	T.Pyriformis toxicity (log ug/L)	Minnow toxicity (log mM)	Lipinski's rule of Five	Bioavailability score (%)
C1	No	0.462	No	No	2.472	0.899	No	Yes	2.197	0.155	No; 2 violations: MW<250, Rotors>7	0.55
C2	No	0.592	No	No	2.55	5.208	No	No	0.285	6.015	No; 1 violation: MW>350	0.17
C3	No	0.626	No	No	2.452	3.135	No	No	0.301	1.99	Yes	0.55
C4	No	-0.35	No	No	2.586	1.667	Yes	No	0.285	0.762	No; 2 violations: MW>350, XLOGP3>3.5	0.56
C5	Yes	-0.084	No	Yes	1.987	1.069	No	No	1.3	0.41	Yes	0.55
C6	No	0.737	No	No	2.366	1.406	No	Yes	0.9	1.235	No; 1 violation: MW<250	0.55
C7	No	1.164	No	No	2.051	1.9	No	No	0.268	2.598	No; 1 violation: MW<250	0.55
C8	No	1.164	No	No	2.213	1.622	No	No	-0.63	2.101	No; 1 violation: MW<250	0.55
C9	No	0.328	No	No	2.45	2.298	No	No	0.38	2.432	Yes	0.55
C10	No	0.577	No	No	2.595	4.635	No	No	0.285	4.897	No; 1 violation: MW>350	0.55
C11	No	0.078	No	No	2.592	0.575	No	No	0.285	1.106	No; 2 violations: MW>350, XLOGP3>3.5	0.56
C12	No	-0.845	No	Yes	2.723	3.566	No	No	0.285	12.274	No; 2 violations: MW>350, Rotors>7	0.17
C13	No	0.144	No	No	2.256	2.206	Yes	No	0.285	-1.174	No; 2 violations: MW>350, XLOGP3>3.5	0.85
C14	No	1.517	No	No	1.65	2.262	No	No	1.084	-0.109	No; 2 violations: Rotors>7, XLOGP3>3.5	0.55
C15	No	1.145	No	No	2.383	2.092	No	No	0.293	2.246	No; 1 violation: MW<250	0.56
C16	No	0.438	No	No	2.428	2.5	No	No	0.347	3.585	Yes	0.55
C17	No	-0.134	No	No	1.973	2.982	No	No	0.285	5.741	No; 1 violation: MW>350	0.11
C18	No	0.124	No	No	2.513	1.858	Yes	No	0.285	0.276	No; 2 violations: MW>350, XLOGP3>3.5	0.56
C19	No	0.582	No	No	2.711	1.857	No	Yes	2.008	0.516	No; 1 violation: MW<250	0.55
C20	No	2.189	No	No	1.581	3.681	Yes	No	0.285	5.62	No; 1 violation: MW<250	0.55
C21	No	0.7	No	No	2.218	3.06	No	No	0.285	3.188	No; 1 violation: MW<250	0.56
C22	No	0.519	No	Yes	2.587	3.228	No	No	0.285	7.155	No; 1 violation: MW>350	0.17
C23	No	0.531	No	No	2.449	2.505	No	No	0.312	2.885	Yes	0.55
C24	No	1.102	No	No	2.168	3.534	No	No	0.285	9.05	No; 2 violations: MW>350, Rotors>7	0.17
C25	No	0.499	No	No	2.455	2.409	No	No	0.326	3.169	Yes	0.55
C26	No	0.085	No	No	2.619	2.672	No	No	0.285	2.123	No; 2 violations: MW>350, XLOGP3>3.5	0.56
C27	No	0.58	No	No	2.396	4.277	No	No	0.285	5.898	No; 1 violation: MW>350	0.17
C28	No	0.499	No	No	2.471	2.612	No	No	0.288	3.721	Yes	0.55
C29	No	-0.001	No	No	2.226	1.567	No	No	0.313	-0.14	No; 2 violations: MW>350, XLOGP3>3.5	0.55
C30	No	0.452	No	Yes	2.491	3.673	No	No	0.285	7.677	No; 1 violation: MW>350	0.17
C31	No	1.319	No	No	1.503	3.137	No	No	0.285	5.592	Yes	0.55
C32	No	0.183	No	No	2.728	3.059	No	No	0.285	3.627	No; 2 violations: MW>350, Rotors>7	0.55
C33	No	1.115	No	No	2.02	2.635	No	No	0.166	2.088	No; 1 violation: MW<250	0.55
C34	No	0.291	No	No	2.355	2.425	No	No	0.287	-0.137	No; 2 violations: MW>350, XLOGP3>3.5	0.56
C35	No	-0.362	No	No	3.006	1.712	No	No	0.294	0.535	No; 3 violations: MW>350, Rotors>7, XLOGP3>3.5	0.56
C36	No	-1.524	No	Yes	2.597	4.079	No	No	0.285	9.202	No; 2 violations: MW>350, Rotors>7	0.17
C37	No	-0.84	No	No	2.181	1.85	No	No	0.497	-0.245	No; 2 violations: MW>350, XLOGP3>3.5	0.55
C38	No	-1.006	No	No	2.479	1.619	No	No	0.341	0.168	No; 2 violations: MW>350, XLOGP3>3.5	0.55

glibenclamide showed a binding score of -8.9 through bounded with TRP-58, TRP-59, GLN-63, HIS-305 and ALA-307 (Figures 6 and 7). In addition, another 9 compounds manifested higher binding affinities than the standard, in particular, compounds 4, 11, 13, 18, 20, 29, 30, 34 and 37 exhibited magnificent binding affinity with values of -9.3, -9, -9,7, -10, -9.1, -9.9, -8.9, -10.5, and -10.5 respectively (Table 2).

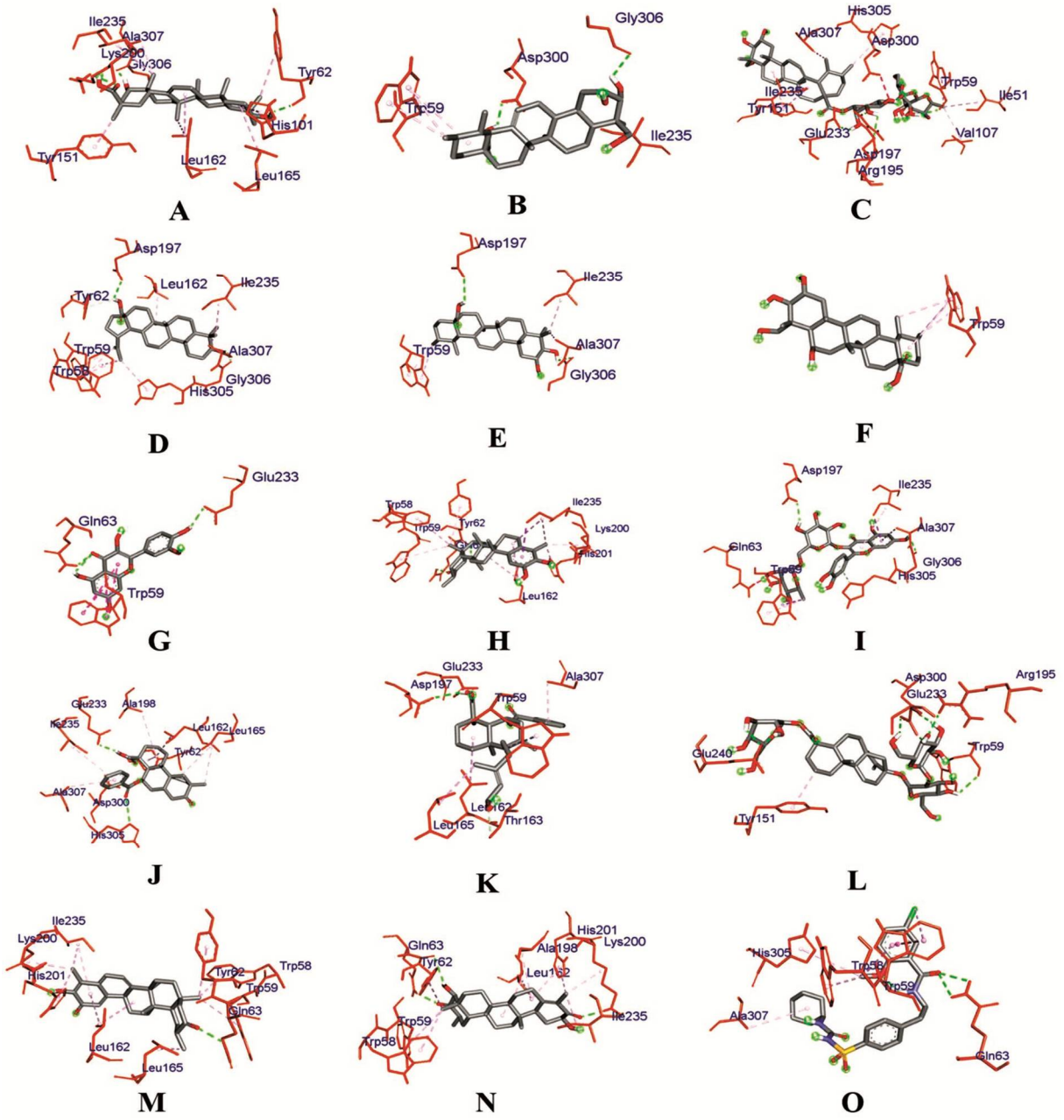

Figure 6**.** Graphical representation of the molecular interactions of the leading phytocompounds with the α-amylase (PDB ID 1HNY) enzyme with 3D visualization (Compound 4 = A, Compound 11 = B, Compound 12 = C, Compound 13 = D, Compound 18 = E, Compound 26 = F, Compound 28 = G, Compound 29 = H, Compound 30 = I, Compound 34 = J, Compound 35 = K, Compound 36 = L, Compound 37 = M, Compound 38 = N, and standard glibenclamide = O).

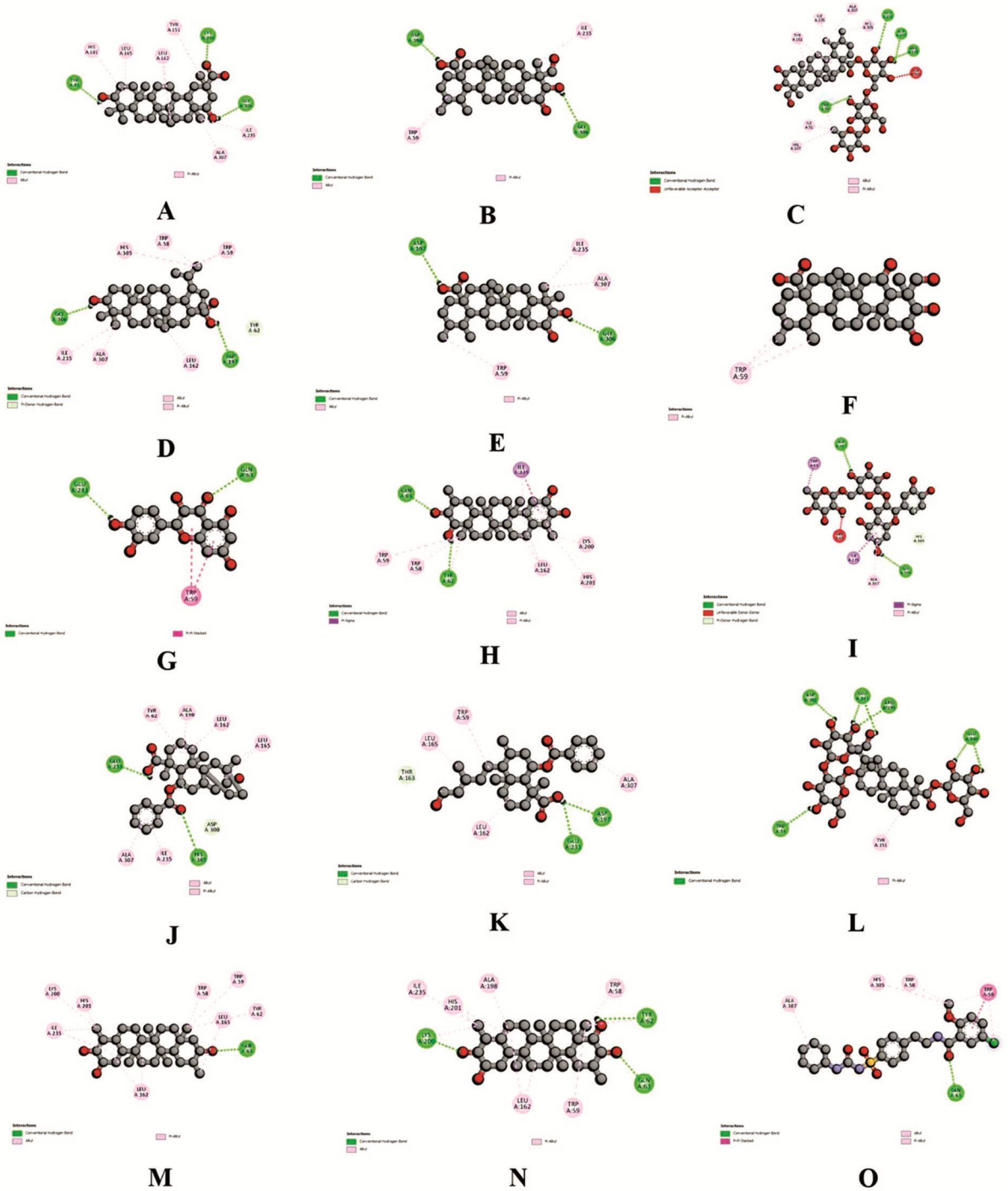

Figure 7. Graphical representation of the molecular interactions of the leading phytocompounds with the α-amylase (PDB ID 1HNY) enzyme with 2D visualization (Compound 4 = A, Compound 11 = B, Compound 12 = C, Compound 13 = D, Compound 18 = E, Compound 26 = F, Compound 28 = G, Compound 29 = H, Compound 30 = I, Compound 34 = J, Compound 35 = K, Compound 36 = L, Compound 37 = M, Compound 38 = N, and standard glibenclamide = O).

Through this study, several compounds have been found to have prominent results against multiple targets, especially compounds 3, 9, 10, 17, 22 and 25 demonstrated magnificent binding against both GLUT-3 and PPARγ receptors, while compounds 4, 34, 36, 37 and 38 showed excellent binding affinity

against PPARγ and α-amylase receptors. Surprisingly compounds 29 and 30 demonstrated potential binding affinity against all of the three receptors suggesting could become prominent drug candidates for further investigation. Thus these compounds went through ADMET and drug-likeliness studies (Tables 3, 4, and 5), both of which violate Lipinski's rule of five, but compound 29 scored a prominent 0.55% in bioavailability while compound poor 0.17 %. Also, compound 29 showed 94.799 % intestinal absorptivity, and was unaffected by most CYP enzymes. This investigation suggests that compound 29 could be a very good drug candidate (Table 5). Following Lipinski's rules of five, a method to assess oral absorption and permeability considerably enhanced the likelihood that hits would be commercially successful, thus, researchers have a tendency to favor hits that adhere to these rules of five (Giménezc *et al.*, 2010). In our study, 8 compounds in particular compounds 3, 5, 9, 16, 23, 25, 26, and 31 follow all of the rules of five. In contrast, other compounds except compound 39 violate the highest 2 rules especially the rules for molecular weight. Though compound 39 violates 3 rules it showed 0.55% bioavailability which is satisfactory. With the exception of 8, all 30 compounds showed promising bioavailability scores of at least 0.55%, including compound 13 displaying the highest bioavailability score of 0.85% (Table 5).

Table 3 demonstrated that all of the substances showed negative values for water solubility (log mol/L) in the pharmacokinetic analysis of absorption, indicating their lipophilic character, which enables effective absorption. The BBB (blood brain barrier) permeability of all of these compounds, with the exception of compounds 1, 37 and 38 was negative, indicating that they are not soluble in the BBB and so will not have any deleterious effects on the central nervous system (CNS). Further compounds 1, 2, 6, 7, 10, 12, 15, 16, 17, 19, 20, 21, 22, 24,27, 30 and 31 showed no binding with any variants of CYP enzyme (Table 4). This result indicates that those compounds will not interact with other drugs related to CYP-enzyme-targeted drugs as well as probably they will not show hepatotoxicity and cardiotoxicity (Hassan *et al.*, 2022). The further investigation explored that (Table 5), none of the compounds inhibit hERG I and most of the compound except only five compounds (5, 12, 22, 30 and 36) does not inhibit hERG II suggesting that these compounds are not cardiotoxic (Muster *et al*., 2008).

The majority of these phytoconstituents appear to have positive antidiabetic actions on these targets, as well as excellent ADMET criteria and drug likelihood, according to this docking.

Conclusion

The preliminary drug discovery study was conducted with 38 phytocompounds by evaluating their binding with three common receptors related to diabetic conditions. Several compounds have conveyed promising results through this study. Also, these compounds manifested good results in their ADMET and drug-likeliness studies which improved their chances to become promising leads for new drug discovery. Moreover, based on the results of this study, we can speculate that the isolated compounds could be the starting points for the development of anti-diabetic therapeutic agents, though the precise mechanism is still unknown. Research should be done to improve semi-synthetic derivatives or develop better medications to treat diabetic conditions.

Declarations

All interested authors have read and approved the article for submission. The entire document has never been published, and it is not currently under consideration for publication in any journal in any portion.

Conflict of interest

There are no competing interests according to the author.

References

Alam, S., Dhar, A., Hasan, M., Richi, F.T., Emon, N.U., Aziz, M., Mamun, A.A., Chowdhury, M., Rahman, N., Hossain, M. and Kim, J.K. 2022. Antidiabetic potential of commonly available fruit plants in bangladesh: updates on prospective phytochemicals and their reported MoAs. *Mol*. **27**, 8709.

Alam, S., Emon, N.U., Hasib, M.S., Rashid, M.A., Soma, M.A., Saha, T. and Haque, M.R. 2021a. Computer-aided approaches to support the ethnopharmaco-logical importance of *Dillenia pentagyna* Roxb.: an *in silico* study. *Bangladesh J. Pharmacol*. **24**, 125-132.

Alam, S., Emon, N.U., Shahriar, S., Richi, F.T., Haque, M.R., Islam, M.N., Sakib, S.A. and Ganguly, A. 2020. Pharmacological and computer-aided studies provide new insights into *Millettia peguensis* Ali (Fabaceae). *Saudi Pharm. J.* **28**, 1777-1790.

Alam, S., Rashid, M.A., Sarker, M.M.R., Emon, N.U., Arman, M., Mohamed, I.N. and Haque, M.R. 2021b. Antidiarrheal, antimicrobial and antioxidant potentials of methanol extract of *Colocasia gigantea* Hook. f. leaves: evidenced from *in vivo* and *in vitro* studies along with computer-aided approaches. *BMC Complement. Med. Ther*. **21**, 1-12.

Alam, S., Sarker, M.M.R., Sultana, T.N., Chowdhury, M.N.R., Rashid, M.A., Chaity, N.I., Zhao, C., Xiao, J., Hafez, E.E., Khan, S.A. and Mohamed, I.N. 2022a. Antidiabetic phytochemicals from medicinal plants: prospective candidates for new drug discovery and development. *Front. Endocrinol*. **13**, 800714.

Amraee, S. and Bahramikia, S. 2019. Inhibitory effect of effective fraction of salvia officinalis on aldose reductase activity: strategy to reduce complications of type 2 diabetes. *Orient. Pharm. Exp. Med*. **19**, 211-216.

Asad, S., Kabir, F., Alam, S., Richi, F.T., Anny, I.P., Nesa, M.L. and Rashid, M.A. 2022. *In vitro* analysis provides new insights into the pharmacological actions of methanol extract of seeds of *Tamarindus indica* L. and its Kupchan fractions. *Bangladesh Pharm. J.* **25**, 9-15.

Ashrafi, S., Rahman, M., Ahmed, P., Alam, S. and Hossain, M. 2022. Prospective Asian plants with corroborated antiviral potentials: position standing in recent years. *Beni-Suef Univ. J. Basic. Appl. Sci* . **11**, 1-26.

Balamurugan, R., Stalin, A. and Ignacimuthu, S. 2012. Molecular docking of γ-sitosterol with some targets related to diabetes. *Eur. J. Med. Chem.* **47**, 38-43.

Becheva, M.S.V. and Kirkova-Bogdanova, A.G. 2022. Prophylactics of type 2 diabetes and diabetic foot. *Iran. J. Public Health*. **51**, 2370.

Chakrabarty, N., Chung, H.J., Alam, R., Emon, N.U., Alam, S., Kabir, M.F., Islam, M.M., Hong, S.T., Sarkar, T., Sarker, M.M.R. and Rahman, M.M. 2022. Chemico-pharmacological screening of the methanol extract of *Gynura nepalensis* DC deciphered promising antioxidant and hepatoprotective potentials: evidenced from *in vitro, in vivo* and computer-aided studies. *Mol.* **27**, 3474.

Chowdhury, M.N.R., Alif, Y.A., Alam, S., Emon, N.U., Richi, F.T., Zihad, S.N.K., Toki, M.T.I. and Rashid, M.A. 2022. Theoretical effectiveness of steam inhalation against SARS-CoV-2 infection: updates on clinical trials, mechanism of actions and traditional approaches. *Heliyon* **8**, 08816.

Emon, N.U., Alam, S., Rudra, S., Al Haidar, I.K., Farhad, M., Rana, M.E.H. and Ganguly, A. 2021b. Antipyretic activity of the leaves extract of *Caesalpinia digyna* Rottl along with phytoconstituent's binding affinity to COX-1, COX-2 and mPGES-1 receptors: *in vivo* and *in silico* approaches. *Saudi J. Biol. Sci.* ***28***, 5302-5309.

Emon, N.U., Alam, S., Rudra, S., Chowdhury, S., Rajbangshi, J.C. and Ganguly, A. 2020a. Evaluation of pharmacological potentials of the aerial part of *Achyranthes aspera* L.: *in vivo*, *in vitro* and *in silico* approaches. *Adv. Tradit. Med*. **22**, 1-14.

Emon, N.U., Rudra, S., Alam, S., Al Haidar, I.K., Paul, S., Richi, F.T., Shahriar, S., Sayeed, M.A., Tumpa, N.I. and Ganguly, A. 2021a. Chemical, biological and protein-receptor binding profiling of *Bauhinia scandens* L. stems provide new insights into the management of pain, inflammation, pyrexia and thrombosis. *Biomed. Pharmacother*. **143**, 112185.

Fan, J., Fu, A. and Zhang, L. 2019. Progress in molecular docking. *Quant. Biol*. **7**, 83-89.

Giménez, B.G., Santos, M.S., Ferrarini, M. and Fernandes, J.P.S. 2010. Evaluation of blockbuster drugs under the rule-of-five. *Die Pharmazie- Int. J. Pharm. Sci*. **65**, 148-152.

Hassan, S.S.U., Abbas, S.Q., Ali, F., Ishaq, M., Bano, I., Hassan, M., Jin, H.Z. and Bungau, S.G. 2022. A comprehensive *in silico* exploration of pharmacological properties, bioactivities, molecular docking and anticancer potential of vieloplain F from *Xylopia vielana* targeting B-Raf kinase. Mol. **27**, 917.

Islam, M.A., Alam, S., Saha, T., Akter, F., Hasnat, H., Zaman, A., Ghosh, S. and Rashid, M.A. 2022a. Evaluation of biological activities of methanolic extract of leaves of *Bruguiera gymnorhiza* (L.) Lam.: *in vivo* studies using swiss albino mice model. *Bangladesh J. Pharmacol*. **25**, 26-31.

Islam, M.M., Alam, R., Chung, H.J., Emon, N.U., Kabir, M.F., Rudra, S., Alam, S., Ullah, A., Hong, S.T. and Sayeed, M.A. 2022b. Chemical, pharmacological and computerized molecular analysis of stem's extracts of *Bauhinia scandens* L. provide insights into the management of diarrheal and microbial infections. *Nutrients* **14**, 265.

Jhong, C.H., Riyaphan, J., Lin, S.H., Chia, Y.C. and Weng, C.F. 2015. Screening alpha-glucosidase and alpha-amylase inhibitors from natural compounds by molecular docking *in silico. Biofactors*, **41**, 242-251.

Kabir, F., Jaman, A.U., Rumpa, R.A., Jannat, T., Alam, S., Saha, T., Islam, M.A. and Soma, M.A. 2021. *In vitro* and *in vivo* investigations provide new insights into bioactivities of *Blumea clarkei* Hook. f. leaves. *Bangladesh Pharm. J.* **24**, 49-158.

Kharroubi, A.T. and Darwish, H.M. 2015. Diabetes mellitus: the epidemic of the century. *World J. Diabetes* **6**, 850-67.

Mahmud, S., Rafi, M., Paul, G.K., Promi, M.M., Shimu, M., Sultana, S., Biswas, S., Emran, T.B., Dhama, K., Alyami, S.A. and Moni, M.A. 2021. Designing a multi-epitope vaccine candidate to combat MERS-CoV by employing an immunoinformatics approach. *Sci. Rep.* **11**, 1-20.

Mojica, L., de Mejia, E.G., Granados-Silvestre, M.Á. and Menjivar, M. 2017. Evaluation of the hypoglycemic potential of a black bean hydrolyzed protein isolate and its pure peptides using *in silico*, *in vitro* and *in vivo* approaches. *J. Funct. Foods* **31**, 274-286.

Morris, G.M. and Lim-Wilby, M. 2008. Molecular docking. In: Kukol, A. (ed) Molecular Modeling of Proteins. Methods Molecular Biology. Humana Preess. Vol **443**, 365-382.

Muster, W., Breidenbach, A., Fischer, H., Kirchner, S., Müller, L. and Pähler, A. 2008. Computational toxicology in drug development. *Drug discov. today* **13**, 303-310.

Obonti, A.T., Alam, S., Kamal, T.B., Zaman, A., Hasnat, H., Saha, T. and Islam, M.A. 2021. Prospective plants with corroborated antimalarial actions: a review. *Bangladesh J. Pharmacol.* **24**, 180-193.

Selvaraj, G., Kaliamurthi, S. and Thirugnanasambandam, R. 2014. Molecular docking studies on potential PPAR-γ agonist from *Rhizophora apiculata*. *Bangladesh J. Pharmacol.* **9**, 298-302.